Clinical Science (2013) **125**, 501–511 (Printed in Great Britain) doi: 10.1042/CS20130064



Original Paper

# Impact of PPAR-$\alpha$ induction on glucose homoeostasis in alcohol-fed mice

Valérie LEBRUN*, Olivier MOLENDI-COSTE*[1], Nicolas LANTHIER*, Christine SEMPOUX*†, Patrice D. CANI‡, Nico VAN ROOIJEN§, Peter STÄRKEL*, Yves HORSMANS* and Isabelle A. LECLERCQ*

*Laboratory of Hepato-Gastroenterology, Institut de Recherche Expérimentale et Clinique (IREC), Université catholique de Louvain, 1200 Brussels, Belgium
†Pathology Department, Cliniques Universitaires Saint-Luc, Université catholique de Louvain, 1200 Brussels, Belgium
‡Louvain Drug Research Institute, Metabolism and Nutrition research group, Université catholique de Louvain, 1200 Brussels, Belgium
§Department of Molecular Cell Biology, Vrije Universiteit Medical Center, 1081 Amsterdam, The Netherlands

## Abstract

Alcohol consumption is a major cause of liver disease. It also associates with increased cardiovascular risk and Type 2 diabetes. ALD (alcoholic liver disease) and NAFLD (non-alcoholic fatty liver disease) share pathological features, pathogenic mechanisms and pattern of disease progression. In NAFLD, steatosis, lipotoxicity and liver inflammation participate to hepatic insulin resistance. The aim of the present study was to verify the effect of alcohol on hepatic insulin sensitivity and to evaluate the role of alcohol-induced steatosis and inflammation on glucose homoeostasis. C57BL/6J mice were fed for 20 days a modified Lieber–DeCarli diet in which the alcohol concentration was gradually increased up to 35% of daily caloric intake. OH (alcohol liquid diet)-fed mice had liver steatosis and inflammatory infiltration. In addition, these mice developed insulin resistance in the liver, but not in muscles, as demonstrated by euglycaemic–hyperinsulinaemic clamp and analysis of the insulin signalling cascade. Treatment with the PPAR-$\alpha$ (peroxisome-proliferator-activated receptor-$\alpha$) agonist Wy14,643 protected against OH-induced steatosis and KC (Kupffer cell) activation and almost abolished OH-induced insulin resistance. As KC activation may modulate insulin sensitivity, we repeated the clamp studies in mice depleted in KC to decipher the role of macrophages. Depletion of KC using liposomes-encapsuled clodronate in OH-fed mice failed both to improve hepatic steatosis and to restore insulin sensitivity as assessed by clamp. Our study shows that chronic alcohol consumption induces steatosis, KC activation and hepatic insulin resistance in mice. PPAR-$\alpha$ agonist treatment that prevents steatosis and dampens hepatic inflammation also prevents alcohol-induced hepatic insulin resistance. However, KC depletion has little impact on OH-induced metabolic disturbances.

**Key words:** alcoholic liver disease, insulin resistance, Kupffer cell, liver steatosis, peroxisome-proliferator-activated receptor-$\alpha$ (PPAR-$\alpha$) agonist

## INTRODUCTION

Excessive ingestion of alcohol is the major cause of chronic liver disease in Western countries. Alcohol consumption ranks third as a cause of premature death and disability in Europe, just after tobacco smoking and high blood pressure [1–3]. Besides the effect on the liver, it is increasingly recognized that alcohol has a very important role in several other diseases, such as cardiovascular diseases, cancer and T2DM (Type 2 diabetes mellitus).

Fatty liver disease induced by alcohol [ALD (alcoholic liver disease)] or arising as a complication of the metabolic syndrome [NAFLD (non-alcoholic fatty liver disease)] [4] share similar histological features, pathological spectrum and disease progression. Oxidative stress and altered hepatic lipid metabolism are key pathogenic factors in the two diseases. Of importance, dysbiosis, increased gut permeability and liver inflammation with, in particular, activation of KCs (Kupffer cells), the liver resident macrophages, are pathogenic determinants of both ALD and NAFLD [5,6].

**Abbreviations:** ACC, acyl-CoA carboxylase; ACO, acyl-CoA oxidase; ALD, alcoholic liver disease; ALT, alanine transaminase; Clo, clodronate; COX-2, cyclo-oxygenase-2; CTL, control liquid diet; ERK, extracellular-signal-regulated kinase; FA, fatty acid; FAS, FA synthase; GIR, glucose infusion rate; GLUT-4, glucose transporter-4; H&E, haematoxylin and eosin; HGP, hepatic glucose production; HSP-90, heat-shock protein-90; ICAM-1, intercellular adhesion molecule-1; IL, interleukin; IR, insulin receptor; KC, Kupffer cell; LFABP, liver FA-binding protein; LPS, lipopolysaccharide; NAFLD, non-alcoholic fatty liver disease; NLRP3, NACHT, LRR and PYD domains-containing protein 3; OH, alcohol liquid diet; PPAR-$\alpha$, peroxisome-proliferator-activated receptor-$\alpha$; qPCR, quantitative real-time PCR; RPL-19, ribosomal protein L19; SOCS-3, suppressor of cytokine signalling 3; SREBP, sterol-regulatory-element-binding protein; TLR, Toll-like receptor; TNF, tumour necrosis factor; TO, turnover.

[1]**Present address:** UMR 1011 (Team 3), Institut Pasteur de Lille, 1 rue du professeur Calmette, BP245–59019–Lille, France.

**Correspondence:** Professor Isabelle A. Leclercq (email isabelle.leclercq@uclouvain.be).

NAFLD is intricately associated with insulin resistance. Low-grade chronic inflammation and activation of pro-inflammatory intracellular pathways are believed to drive insulin resistance in this context. Metabolic overload causes oxidative stress and accumulation of lipotoxic species that trigger a stress response involving kinases such as JNK (c-Jun N-terminal kinase), PKC (protein kinase C) and NF-$\kappa$B (nuclear factor $\kappa$B) contributing to inhibition of insulin-dependent signal [4,6–8]. Systemic inflammation and in particular inflammation of the obese adipose tissue are essential components, as numerous studies have shown that reduction of adipose tissue inflammation ameliorates hepatic steatosis and insulin resistance [9]. Inside the liver, activation of the KCs also participates in hepatic insulin resistance, and KC depletion has been shown to prevent hepatic insulin resistance caused by high fat feeding [10].

Given the pathological and pathogenic similarities between ALD and NAFLD, the question arises as to whether insulin signalling might also be perturbed and participate in disease progression in ALD. A diabetogenic effect has been attributed to heavy alcohol consumption contributed to by excess calorie intake, impairment of insulin production by pancreatic $\beta$-cells [caused by alcohol-induced ER (endoplasmic reticulum) stress] and induction of pancreatitis [11]. Alcohol has also been reported to cause insulin resistance, but the underlying mechanisms remain poorly investigated. Chronic alcohol consumption in both humans and rodents decreases whole-body glucose utilization during hyperinsulinaemic euglycaemic clamp [12]. OH (alcohol liquid diet)-induced steatosis may alter insulin signalling as mentioned above. Studies in rats have demonstrated that chronic alcohol consumption was associated with increased macrophage infiltration in the adipose tissue and changes in the expression of adipocytokines. This leads to insulin resistance in the adipose tissue and decreased inhibition of lipoprotein lipase, which contributes to increased NEFA [non-esterified 'free' FA (fatty acid)] delivery to the liver and hence to steatosis [12] and possibly to hepatic insulin resistance.

Studies in rats have clearly demonstrated that the activation of KC plays a crucial role in ALD [13–15] as KC depletion prevents most of the liver alterations caused by alcohol [16–18]. Alcohol provokes gut dysbiosis and increased gut permeability, thereby increasing the levels of bacterial by-products [LPS (lipopolysaccharide), peptidoglycans, etc.] in the portal blood. Those, upon binding to TLR (Toll-like receptor), activate KC and stimulate production of pro-inflammatory cytokines. Alcohol also sensitizes KC to LPS by increasing oxidative stress and prime KC to respond to TLR ligands by up-regulating a number of pro-inflammatory molecules and receptors [5,19,20]. Indeed, treatment with prebiotics that reduced bacterial overgrowth, gut permeability and endotoxaemia lessened alcoholic steatohepatitis [21], whereas TLR4-KO mice were protected from OH-induced steatosis [22].

The aim of the present study is to progress in our understanding of the mechanisms of alcohol-induced insulin resistance. We showed that PPAR-$\alpha$ (peroxisome-proliferator-activated receptor-$\alpha$) stimulation prevented OH-induced steatosis and, in turn, hepatic insulin resistance.

## MATERIALS AND METHODS

### Animal model

Female 8-week-old C57BL/6 J mice bred in our animal house facility were exposed to a 12-h light/12-h dark cycle and maintained at a constant temperature of 20–22 °C. Animal care was provided in accordance with the guidelines for humane care for laboratory animals established by the Université catholique de Louvain in accordance with European regulations, and the study protocol was approved by the university ethics committee.

### Ethanol feeding

Ethanol-fed mice had free access to a liquid diet containing alcohol (Lieber–DeCarli liquid diet; BioServ) as the sole source of food and drink (OH group, $n = 15$) and food intake was monitored daily. Control mice were pair-fed a CTL (control liquid diet) in which alcohol was isocalorically substituted by dextrimaltose. Pair-fed mice were given the same volume of food as their ethanol-fed counterparts consumed during the preceding 24 h (pair-fed controls, $n = 10$). Control and OH diet contain 35% of energy as lipids. Liquid diets were dispensed through glass liquid-diet feeding tubes (BioServ) and replaced each day. Following a 2-day habituation period to the liquid diet, ethanol was added to the diet and its concentration gradually increased every second day (with 4, 8, 16, 28 and 35% of energy intake as alcohol). Alcohol at 35% was maintained for 10 days [see Figure 1(A) for a schematic representation of the experimental protocol]. The total duration of OH-feeding was 20 days. All experiments were run on two sets of animals: one used for tissues and samples collection, whereas euglycaemic hyperinsulinaemic clamp studies were performed on the other.

### Sample preparation

At the time of kill, mice were anesthetized with ketamine/xylazin and 5 international units of insulin (Actrapid®) or an equal volume of PBS were directly injected into the portal vein. At 1 min after the injection, the blood was drawn by cardiac puncture and plasma prepared and stored until use. In some animals, blood was drawn in apyogenic conditions, the plasma prepared and used for determination of LPS concentrations. The liver, the epididymal adipose tissue and quadriceps were then rapidly dissected out. A part of the liver was immediately immersed in 4% (v/v) formalin for histological analyses. The rest of liver and the other tissues were snap-frozen in liquid nitrogen and kept at − 80 °C until analyses.

### Euglycaemic–hyperinsulinaemic clamp studies

An intrafemoral catheter was implanted upon anaesthesia 1 week prior to the end of the feeding experiment, and insulin sensitivity was assessed by the euglycaemic–hyperinsulinaemic clamp, as described previously [10,23]. Briefly, after 5 h fasting, mice were infused with insulin at a rate of 2.5 m-units/kg of body weight per min for 2.5 h and with glucose at a variable flow rate to maintain euglycaemia [GIR (glucose infusion rate)]. [3-$^3$H]Glucose (PerkinElmer) was infused at a rate of 0.33 $\mu$Ci/min for glucose TO (turnover) measurements.

 

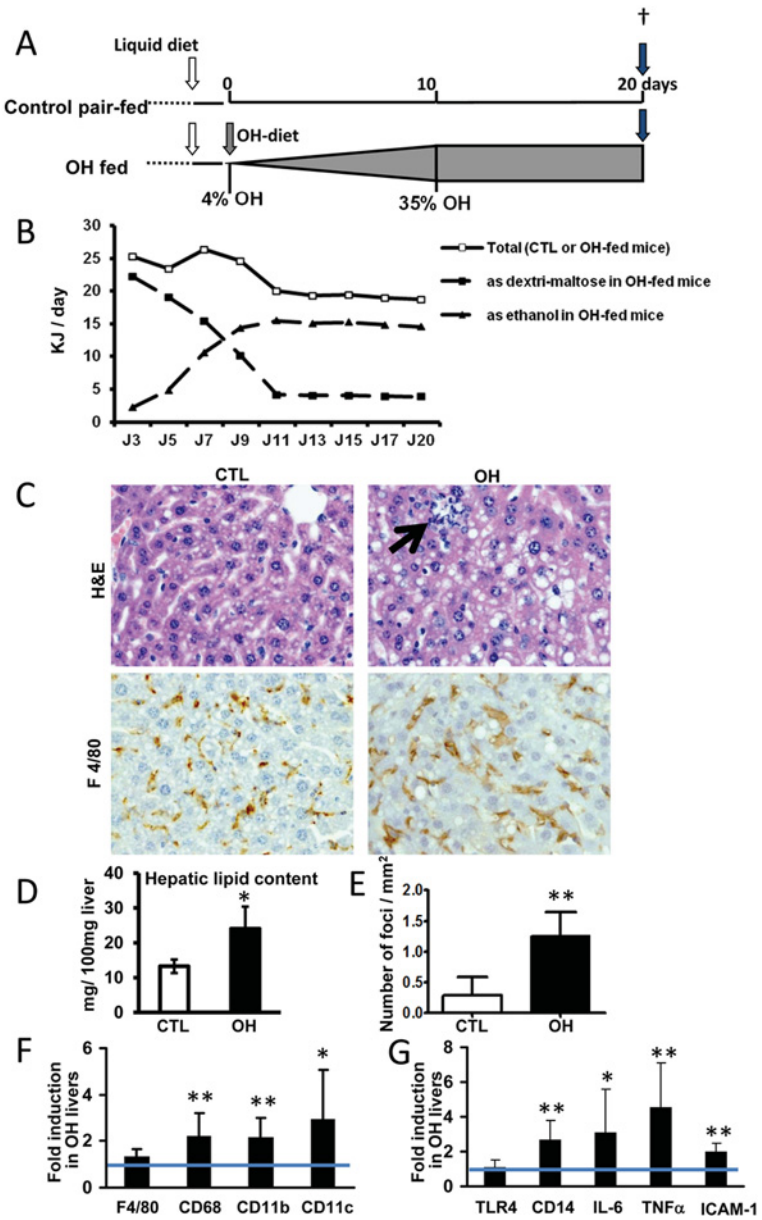


**Figure 1** **OH-feeding induces liver injury**

(**A**) Following a 2-day habituation period to a liquid diet, OH-fed animals were provided *ad libitum* a diet containing ethanol. Its concentration started at 4% of energy as alcohol, gradually increased every two days (8, 16, 28 and 35%) and maintained at 35% for 10 days. Controls were pair-fed for the entire duration (20 days) of the OH protocol: they were provided with a volume of isocaloric liquid diet matching the amount of food consumed by OH-fed mice during the preceding 24 h. (**B**) Mean daily caloric intake in mice fed the OH-diet or pair-fed the control diet (white squares, continuous line), and daily intake of calories from dextri-maltose (black squares, dotted line) and ethanol (black triangles, dotted line) in OH-fed mice. (**C**) H&E staining (original magnification ×40) and F4/80 immunohistochemistry (original magnification ×40) on liver sections from pair-fed control and OH-fed mice. Arrow points towards an inflammatory infiltrate. (**D**) Total liver lipid content and (**E**) number of inflammatory foci (containing more than five inflammatory cells) per $mm^2$ of liver section in pair-fed controls and OH-fed mice. Expression of (**F**) markers of pro-inflammatory cells and (**G**) pro-inflammatory markers in the livers of OH-fed mice relative to that in the livers of CTL-fed arbitrarily set at 1. $*P < 0.05$ and $**P < 0.01$ compared with CTL mice.

## PPAR-$\alpha$ agonist treatment and macrophage depletion

For the PPAR-$\alpha$ agonist study, Wy14,643 (Bio-Connect) was added or not to the liquid control or OH diet at the concentration 12 mg/100 ml, so that mice received a daily dose of ≈1 mg of Wy14,643. To deplete macrophages, liposome-encapsulated Clo (clodronate) (1 mg/ml, 100 $\mu$l/10 g of body weight) or an equal volume of PBS was injected via the retro-orbital plexus as previously reported [10]. Injections started 2 days after the onset of alcohol-feeding and were repeated every 5 days (four

injections/mouse in total), the last injection being performed 2 days before the clamp. Clo (a gift from Roche) was encapsulated into liposomes as described previously [24].

*Histology*

Formalin-fixed and paraffin-embedded tissue was cut in 5-$\mu$m-thick sections. H&E (haematoxylin and eosin) staining and F4/80 immunostaining for identification of KCs were performed according to standard procedure using anti-F4/80 antibody (1:200 dilution; Serotec), a rabbit anti-rat Ig antibody (1:200 dilution; Dako) and a streptavidin–HRP (horseradish peroxidase)-conjugated goat anti-rabbit antibody (En Vision; Dako) [25]. Inflammatory foci, containing more than five inflammatory cells, were counted on one H&E-stained liver section per animal (mean surface = 25 mm$^2$) in five animals per group.

## Biochemical analyses

Blood glucose concentration was determined with a glucose monitor (Accu-chek Aviva; Roche Diagnostics) and plasma insulin concentration with a commercial ELISA kit (Mercodia). Serum transaminase and blood alcohol concentrations were measured using automated techniques (Department of Bio-Medical Chemistry, St Luc University Hospital, Brussels, Belgium). Blood LPS concentration was determined by the LAL (limulus amebocyte lysate) method using the endosafe®-PTS cartridge system (Charles River), according to the manufacturer's instructions, as described previously [26].

Total liver lipids were extracted with methanol and chloroform and quantified using the vanillin–phosphoric acid reaction as described previously [27].

## RNA extraction, reverse transcription and qPCR (quantitative real-time PCR)

Total RNA was extracted from frozen liver samples using TRipure Isolation Reagent (Roche Diagnostics). cDNA was synthetized from 1 $\mu$g of RNA using random hexamers and M-MLV reverse transcriptase (Invitrogen). qPCR analysis was performed as described previously [28]. Primer pairs for transcripts of interest [F4/80, TNF (tumour necrosis factor)-$\alpha$, IL (interleukin)-6, TLR-4, CD11b, CD11c, CD14, CD68, FAS (FA synthase), SREBP-1 (sterol-regulatory-element-binding protein-1), SCD-1 (stearoyl-CoA desaturase-1), ChREB (carbohydrate-responsive element-binding protein), GPAT-1 (glycerol-3-phosphate acyltransferase-1), DGAT-2 (diacylglycerol acyltransferase-2), PPAR-$\alpha$, CD36, ICAM-1 (intercellular adhesion molecule 1), ACO (acyl-CoA oxidase), RPL-19 (ribosomal protein L19), NLRP3 (NACHT, LRR and PYD domains-containing protein 3), ACC (acetyl-CoA carboxylase), LFABP (liver FA-binding protein), IL-1 and SOCS-3 (suppressor of cytokine signalling 3)] were designed using primer express design software and are listed in Supplementary Table S1 (http://www.clinsci.org/cs/125/cs1250501add.htm). The relative amount of transcripts was normalized to the level of expression of RPL19 mRNA, taken as an invariant control and results expressed as fold expression relative to the expression in the control group using the $\Delta\Delta C_t$ method.

## Insulin signalling pathway by Western blotting

Liver wedges were homogenized in a lysis buffer [50 mM Hepes, 150 mM NaCl, 10% (v/v) glycerol, 150 mM $MgCl_2$ and 10% (v/v) Triton X-100] and the resulting homogenate clarified by centrifugation. Proteins were analysed by Western blotting using antibodies and conditions listed in Supplementary Table S2 (http://www.clinsci.org/cs/125/cs1250501add.htm).

## Statistical analysis

All the data are presented as mean $\pm$ S.D. Groups were compared using Student's *t* test. Statistical significance was assumed for *P* values $<0.05$.

# RESULTS

## Chronic alcohol feeding induces hepatic steatosis with KC activation

As per the pair feeding design, energy intake was similar in OH-fed and pair-fed CTL mice during the entire duration of the OH-feeding experiment (Figure 1B). Although body weight remained stable during the first 2 weeks of the feeding experiment, OH-fed animals lost weight during the last week (Table 1). Blood alcohol levels and hepatic expression of CYP2E1 (cytochrome P450 2E1) protein (Table 1) confirmed appropriate ethanol intake in OH-fed animals [19,29].

Compared with CTL-fed mice, OH-fed mice had a higher liver weight, an increased liver-to-body weight ratio but no significant change in the serum ALT (alanine transaminase) levels (Table 1). Histologically, the hepatocytes in zones 2 and 3 of CTL livers contained very small lipid droplets. Livers from OH-fed mice exhibited steatosis with large vesicles displacing the nucleus and enlarging the hepatocytes, more prominently in acinar zones 1 and 2 (Figure 1C). Consistently, the total hepatic lipid content was two times higher in OH-fed than in CTL-fed mice (Figure 1D).

OH-feeding induced liver inflammation as demonstrated by the presence of numerous inflammatory foci (Figures 1C and 1E).We observed that KCs are enlarged in OH-fed animals but not more numerous (Figure 1C). Consistently, hepatic expression of F4/80 was similar in both groups (Figure 1F), whereas the expression of CD68, a glycoprotein expressed by activated KCs, and CD11c, expressed by a subset of activated KCs as well as by monocytes and recruited macrophages, was up-regulated in livers of OH-fed animal, supporting KC activation. Increased expression of CD11b was also consistent with increased recruitment of neutrophils. Although hepatic TLR4 expression was not affected by alcohol feeding, CD14, acting as a co-receptor for TLR4 activation by LPS, was significantly up-regulated in livers of OH-fed mice (Figure 1G). The expression of IL-6, TNF and ICAM-1 was also significantly up-regulated in livers of OH-fed mice (Figure 1G).

## Hepatic insulin resistance is associated with chronic alcohol feeding

We evaluated glucose homoeostasis and insulin sensitivity in OH-fed animals. Despite receiving isocaloric diets, carbohydrate

 

**Table 1 Effect of OH feeding on biometric and histological variables**

Values are means ± S.D. (min value–max value). Pair-fed controls (CTL) ($n = 10$) and OH-fed mice (OH) ($n = 8$); *$n = 5$ and $n = 4$ in CTL and OH respecitvely. NS, not significant.

| Parameter | Pair-fed CTL | OH | *P* value |
|---|---|---|---|
| Body weight (g) | | | |
| Day 0 | 18.5 ± 1.1 | 18.7 ± 0.9 | NS |
| Day 14 | 18.3 ± 0.9 | 18.4 ± 0.8 | NS |
| Day 21 | 18.8 ± 1.1 | 17.0 ± 1.3 | <0.01 |
| Liver weight (g) | 0.77 ± 0.09 | 1.00 ± 0.09 | <0.001 |
| Liver/body weight (%) | 4.09 ± 0.45 | 5.92 ± 0.59 | <0.001 |
| ALT (international units/l) | 23.2 ± 7.9 | 40.7 ± 22.1 | NS |
| Serum LPS (endotoxin units/ml) | 1.25 ± 0.22 (0.62–2.01) | 5.91 ± 2.99 (0.88–17.84) | NS |
| Blood alcohol (g/l) | (0–0.05) | 1.10 ± 0.80 (0.25–1.97) | NS (0.07) |
| Hepatic Cyp2E1 protein | 15.52 ± 0.83 | 26.47 ± 2.50 | <0.01 |
| Glycaemia (mg/dl) | 136 ± 26 | 94 ± 35 | <0.05 |
| Serum insulin ($\mu$g/ml)* | 0.39 ± 0.31 | 0.76 ± 1.36 | NS |

intake was lower in OH-fed than in pair-fed CTL mice as maltose was gradually replaced by ethanol (Figure 1B). Compared with pair-fed controls, blood glucose levels were decreased and serum insulin levels, although highly variable, tended to be increased in OH-fed mice (Table 1).

We used the gold standard euglycaemic–hyperinsulinaemic clamp technique to explore insulin sensitivity *in vivo*. This revealed that insulin resistance in OH-fed mice, as GIR required for maintaining euglycaemia (5.5 mM) in the face of constant insulin infusion, was reduced in OH compared with controls (Figure 2A). We also found that OH-fed mice exhibited hepatic insulin resistance as, unlike in pair-fed control mice, insulin failed to completely inhibit HGP (hepatic glucose production) in OH-fed mice. Hepatic insulin resistance was confirmed by Western blot: insulin-induced phosphorylation of the IR (insulin receptor) was reduced in OH-fed compared with controls. Consistently, a decreased phosphorylation of downstream Akt (on both $Ser^{473}$ and $Thr^{308}$) and ERK (extracellular-signal-regulated kinase) was observed (Figure 2B). In addition, SOCS-3 gene expression, a factor shown in other studies to be able to interact with the IR and prevent its phosphorylation [30,31], was increased in livers from OH-fed mice (1.94 ± 0.69 compared with 1.08 ± 0.53 arbitrary units; $P = 0.014$).

OH-fed mice exhibited decreased glucose TO during clamp studies (Figure 2A). This may translate into decreased glucose uptake by peripheral tissues. We therefore evaluated insulin signalling in skeletal muscle and analysed the adipose tissue. Insulin-driven phosphorylation of IR, Akt and ERK was as high or higher in skeletal muscles of OH-fed animals than in pair-fed controls (Figure 2C), indicating insulin hyper-sensitivity as also reported by others in rats exposed to alcohol [12]. By contrast, GLUT-4 (glucose transporter-4) mRNA expression was decreased in the adipose tissue of OH-fed mice (Figure 2D), whereas the expression of MCP-1 (macrophage chemoattractant protein-1), CD14 and TNF tended to increase (Supplementary Figure S1 at http://www.clinsci.org/cs/125/cs1250501add.htm)], which is consistent with alcohol-induced insulin resistance and inflammation in this tissue.

## Steatosis and insulin resistance

Steatosis may induce hepatic insulin resistance via lipotoxicity. Impairment of $\beta$-oxidation of FAs participates in steatosis upon chronic alcohol exposure [14,32,33]. We therefore used Wy14,643, a potent agonist of PPAR-$\alpha$, the master transcription factor regulating lipolytic pathways, to prevent liver lipid accumulation in OH-fed mice [33] and performed clamp studies to determine the role of hepatic lipids in inducing hepatic insulin resistance in this model. As consistently reported previously [34], administration of Wy14,643 increased liver weight and liver/body weight ratio in both controls (9.21 ± 0.78 compared with 4.85 ± 0.13 %; $P \leqslant 0.001$) and OH-fed animals (12.30 ± 1.06 compared with 5.35 ± 0.39 %; $P \leqslant 0.001$). Despite this, Wy14,643 treatment almost completely prevented alcohol-induced steatosis as visualized on liver histology and confirmed by measurement of hepatic lipid content (Figures 3A and 3B). The PPAR-$\alpha$ agonist treatment was associated with increased expression of ACO, the rate-limiting enzymes for mitochondrial FA oxidation, LFABP and CD36, which facilitate the transport of FA between outer and inner mitochondrial leaflets (Figure 3C). The expression of lipogenic genes (SREBP, FAS and ACC) was not significantly altered (results not shown).

Wy14,643 treatment did not modify insulin sensitivity in mice fed the CTL. By contrast, Wy14,643 improved hepatic insulin resistance caused by OH-feeding as the GIR was similar in Wy14,643-treated OH-fed mice and controls (Figure 3D). This was owing to the restoration of inhibition of hepatic glucose output by insulin. In keeping, Wy14,643 treatment increased insulin-mediated phosphorylation of the IR and downstream AKT ($pThr^{308}$ and, to a lower extent, $pSer^{473}$) in OH-fed animals (Figure 3E).

Besides up-regulating genes of lipid transport and metabolism, PPAR-$\alpha$ also exerts anti-inflammatory effects, partly by acting as a negative regulator of the pro-inflammatory transcription factor NF-$\kappa$B [35]. Consistently, we observed that Wy14,643 treatment to OH-fed animals decreased the expression of COX-2 (cyclo-oxygenase-2), adhesion molecule ICAM-1, inflammatory cytokines IL-1$\beta$ and IL-6 as well as the NRLP3 component

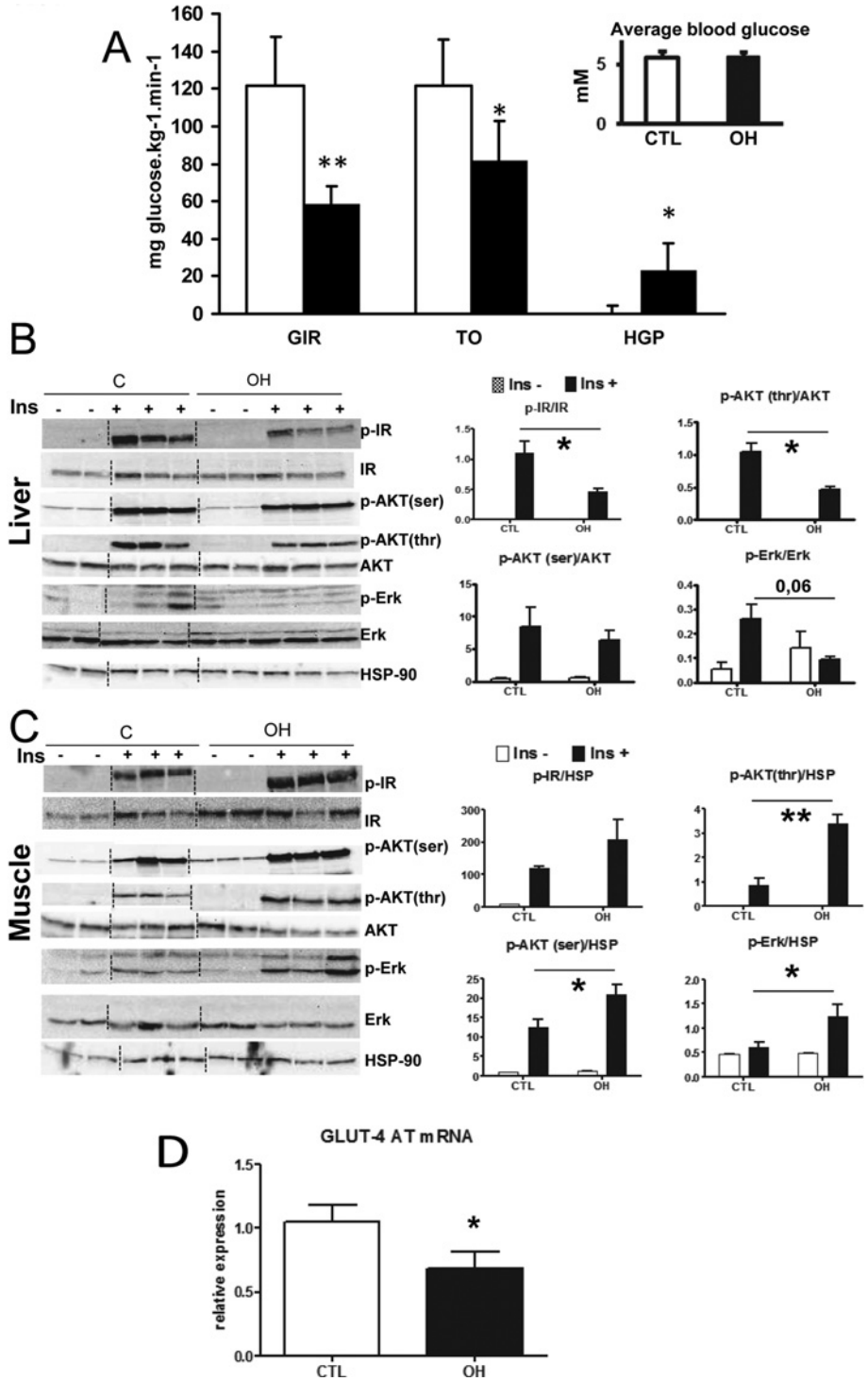


**Figure 2 OH-feeding induces hepatic insulin resistance**

(**A**) GIR, glucose TO and HGP during hyperinsulinaemic–euglycaemic clamps in mice fed the OH diet (dark bars) or pair-fed the control diet (open bars). In the inset graph, mean glycaemia during the 90 min clamping period. Liver (**B**) and muscle (**C**) protein expression and insulin-stimulated phosphorylation of IR, Akt and ERK evaluated by Western blot analysis. HSP-90 (heat-shock protein-90) was used to evaluate loading control. Mice were injected with insulin (Ins +, 5 units, dark bars) or saline (Ins-, open bars). Representative blots and quantification of the ratio of the insulin-stimulated phospho-protein of interest to total protein or invariant HSP-90, as measured by densitometric analysis ($n = 3$–5 per group and condition), are shown. (**D**) GLUT-4 mRNA expression in adipose tissue from mice fed the OH-diet (dark bars) or pair-fed the control diet (open bar). Results are expressed as mean ± S.D. ($n = 4$ per group).*$P < 0.05$ and **$P < 0.01$ compared with control-fed mice.

 

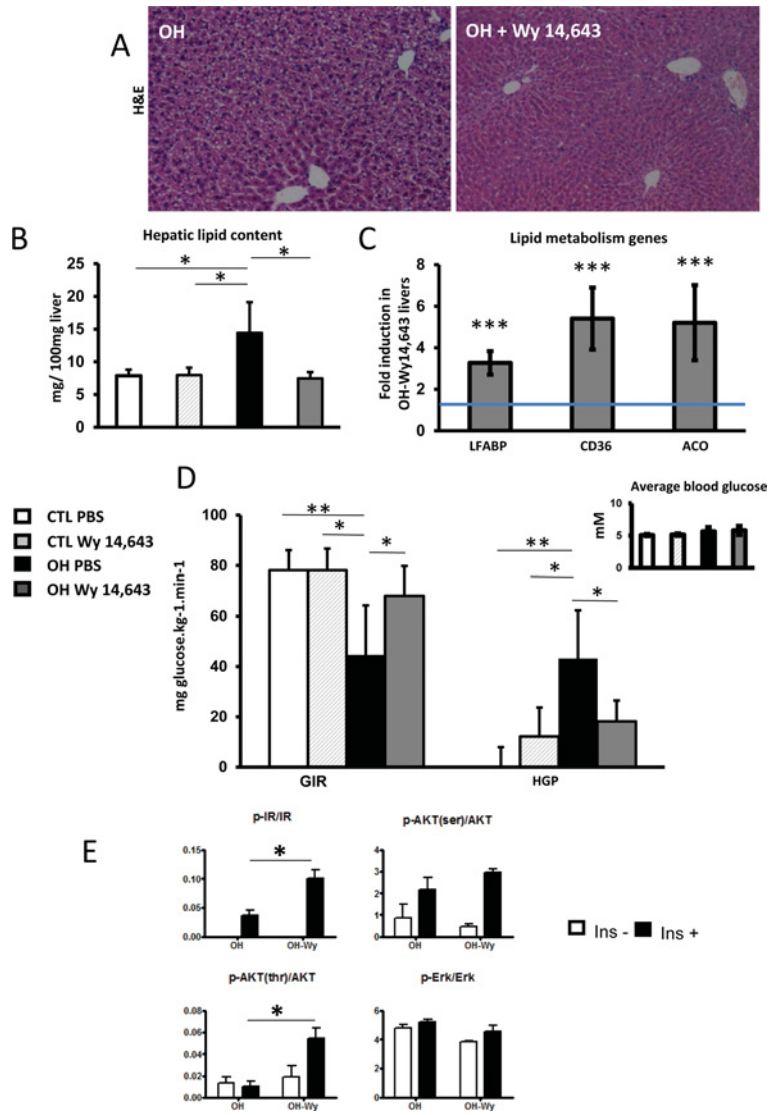


**Figure 3** **Wy14,643 treatment prevents steatosis and improves hepatic insulin sensitivity in OH-fed mice**

(**A**) H&E-stained liver sections from OH-fed mice treated (OH + Wy) or not (OH) with Wy14,643. (**B**) Hepatic lipid content in CTL and OH-fed mice treated or not with Wy14,643. (**C**) Hepatic expression of lipid metabolic genes in Wy14,643-treated, OH-fed mice relative to that of OH-fed mice, arbitrarily set at 1. (**D**) GIR and HGP during hyperinsulinaemic–euglycaemic clamps in pair-fed control (open bars), pair-fed control Wy14,643-treated (hatched bars), OH-fed (dark bars) and OH-fed Wy14,643-treated mice (grey bars). In the inset, mean glycaemia during the 90 min clamping. (**E**) Phosphorylation of IR, Akt and ERK as determined by Western blot analysis in OH-fed mice treated or not with Wy14,643: mice were injected with insulin (Ins +, 5 units, dark bars) or saline (Ins-, open bars). The ratio of the insulin-stimulated phospho-protein of interest to total protein as measured by densitometry analysis are shown ($n = 3$–5 per group and condition). Results are expressed as mean ± S.D. $^{*}P < 0.05$, $^{**}P < 0.01$ and $^{***}P < 0.001$ for comparisons indicated on the graphs.

of the inflammasome (Figure 4A). Further supporting an anti-inflammatory effect, several markers of activated macrophages and inflammatory cells such as F4/80, CD68, CD11c, CD11b and CD14, up-regulated in the livers of OH-fed mice, were reduced upon Wy14,643 treatment (Figure 4B).

## Effect of KCs depletion on insulin sensitivity in alcohol-induced steatohepatitis

Reduced liver fat and decreased liver inflammation may both contribute to improved insulin sensitivity in Wy14,643-treated OH-fed mice. To directly address the contribution of KC in this process, we performed clamp studies in mice depleted in KC for the whole duration of the alcohol-feeding experiment by mean of intravenous injections of liposome-encapsulated Clo [10,36] (Figure 5A). This treatment has no detrimental effect on body weight evolution, alcohol consumption and glycaemia (Supplementary Table S3 at http://www.clinsci.org/cs/125/cs1250501add.htm)]. F4/80 mRNA expression was reduced by 80% in the livers of Clo- compared with PBS-treated OH-fed mice (Figure 5B), confirming significant KC removal. KC

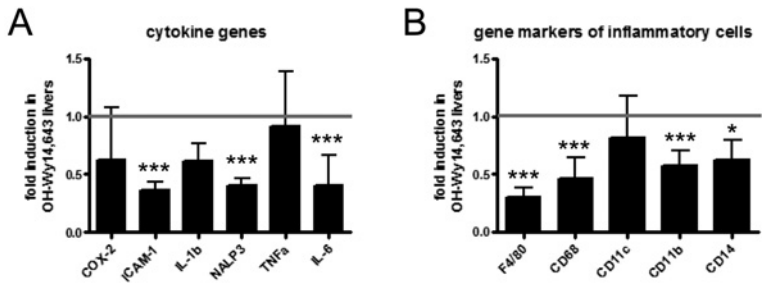


**Figure 4 Wy14,643 treatment reduces liver inflammation in OH-fed mice**
Hepatic expression of cytokine gene (**A**) and gene markers of inflammatory cells (**B**) in Wy14,643-treated, OH-fed mice relative to that of the OH-fed mice, arbitrarily set at 1. Results are expressed as mean ± S.D. $*P < 0.05$, $**P < 0.01$ and $***P < 0.001$ for comparisons indicated in the graphs.

depletion had no impact on liver weight or steatosis, and total lipid content was similar in the two groups (Figure 5C). Repeated injections of PBS–liposomes did not alter the response to OH and, as in untreated mice (Figure 2A), OH decreased GIR and glucose TO and increased HGP in liposome PBS-treated mice (Figure 5D). KC depletion in OH-fed mice had no effect on GIR, and marginally lowered glucose TO and HGP (Figure 5D).

## DISCUSSION

Chronic alcohol feeding at escalating concentration up to 35% for 20 days disrupts glucose homoeostasis as evidenced by decreased whole body insulin sensitivity during hyperinsulinaemic–euglycaemic clamp. Insulin-stimulated tissue glucose uptake and inhibition of HGP are impaired upon alcohol exposure. We report in the present study that PPAR-$\alpha$ agonist treatment that prevents steatosis and dampens hepatic inflammation also prevents alcohol-induced hepatic insulin resistance. However, KC depletion has little impact on metabolic disturbances.

Previous studies in rats have reported that alcohol decreases tissue glucose utilization [12,37,38]. Work by Kang et al. [12] further established that glucose uptake by the adipose tissue but not by skeletal muscles was impaired by alcohol. Consistently, we show that in mice also alcohol feeding decreases glucose utilization. Moreover, dampening of GLUT-4 expression in the adipose tissue together with supra-normal insulin-stimulated signalling in skeletal muscle also support that the adipose tissue is the main contributor to decreased glucose uptake. Inflammatory changes in the adipose tissue, also observed in the rat model, represent a plausible mechanism for alcohol-induced adipose insulin resistance. Increased adipose TLR4/CD14 expression suggests that enhanced susceptibility to a pro-inflammatory gut-derived factor such as LPS may represent a plausible link between alcohol and adipose tissue inflammation [39].

Besides the adipose tissue, the liver is another important compartment contributing to alcohol-induced disturbances of glucose homoeostasis. Indeed, ethanol feeding caused hepatic insulin resistance as it impaired the ability of insulin to inhibit HGP *in vivo* and inhibits hepatic insulin signalling.

Several mechanisms may converge to inhibit hepatic insulin signalling [31]: among those, intra-hepatic fat accumulation and thus lipotoxicity on the one hand, and inflammation and activation of pro-inflammatory pathways on the other hand, are suspected to be prominent players in inducing hepatic insulin resistance in non-alcoholic metabolic contexts such as obesity and NASH (non-alcoholic steatohepatitis) and are also potentially relevant in the alcoholic liver.

Down-regulation and/or dysfunction of PPAR-$\alpha$ appear as major contributors to alcohol-induced steatosis with protection conferred by PPAR-$\alpha$ agonist [33], while PPAR$\alpha$-null mice were exquisitely sensitive to alcohol-induced liver injury, cell death and fibrosis [40]. We therefore evaluated the effect of PPAR-$\alpha$ agonist Wy14,643 on OH-induced hepatic insulin resistance. In our model, PPAR-$\alpha$ agonist significantly improved glucose homoeostasis. In the clamp study, treatment with the agonist restored the whole-body insulin sensitivity (normalization of GIR), through amelioration of hepatic insulin sensitivity, which was also supported by improved insulin-mediated activation of the IR and downstream signalling cascade.

PPAR-$\alpha$ is the major orchestrator of lipid oxidation but also a repressor of pro-inflammatory transcription factor NF-$\kappa$B [32,35]. PPAR-$\alpha$ agonist treatment induced FA-oxidizing genes and decreased fat accumulation and thereby may reduce lipotoxicity. Besides this effect on lipid, Wy14,643 treatment also resulted in decreased inflammation. Activation of KCs and activation of NF-$\kappa$B-regulated pro-inflammatory factors such COX-2, chemoattractant ICAM-1, IL-6, IL-1$\beta$ and the NLRP3 component of the inflammasome, were all attenuated in the livers alcohol-fed mice treated with the PPAR-$\alpha$ agonist. Both reduced lipid accumulation and anti-inflammatory properties may thus co-operate to prevent OH-induced insulin resistance. In order to further explore the mechanisms of OH-induced insulin resistance, we performed KC depletion experiments. KCs are of particular importance in ethanol-induced liver injury. Chronic ethanol exposure sensitizes KCs to LPS [29]. This sensitization enhances the production of various pro-inflammatory mediators, such as TNF, IL-6 or IL1$\beta$ and ROS (reactive oxygen species) that can contribute to hepatocyte dysfunction. Alcohol-associated liver injury is inhibited when endotoxaemia is decreased [21,41], TLR4 or CD14 inactivated [22,42] or KC depleted [16]. In our

 

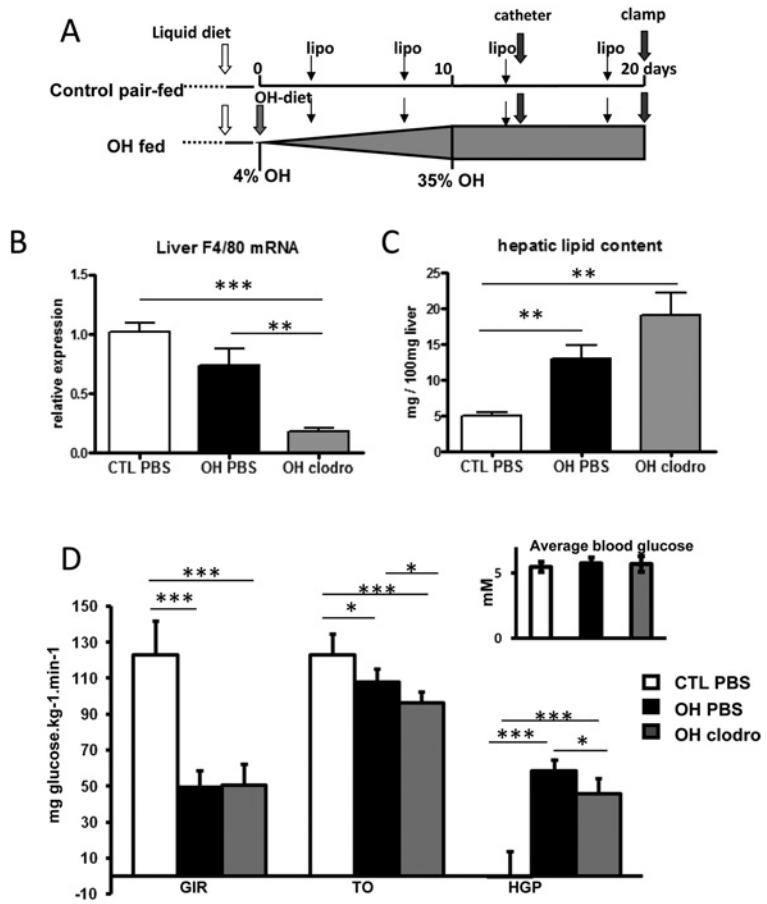


**Figure 5** **KC depletion does not improves OH-induced insulin resistance**

(**A**) CTL-fed and OH-fed mice were injected with Clo- or PBS-loaded liposomes on days 4, 9, 14 and 19 of the feeding protocol. (**B**) Hepatic F4/80 mRNA expression, (**C**) total liver lipid content and (**D**) GIR, glucose TO and HGP during hyperinsulinaemic–euglycaemic clamps in PBS–liposome-treated pair-fed control (open bars), PBS–liposomes-treated OH-fed (dark bars) and clordonate liposome-treated OH-fed (grey bars) mice. The inset shows the mean glycaemia during the 90 min clamping period. Results are expressed as mean $\pm$ S.D. ($n = 4$ per group). $*P < 0.05$, $**P < 0.01$ and $***P < 0.001$ for comparisons indicated on the graphs.

hands, KC depletion by means of repeated injections of liposome-encapsulated Clo, inducing suicide of phagocytic macrophages of the reticulo-endothelial system, did not alter the alcoholization of the mice, nor hepatic steatosis. Depletion of liver macrophage had only marginal consequences for alcohol-induced perturbation of glucose homoeostasis as, as assessed by clamp studies, it failed to modify whole-body insulin sensitivity and only marginally improved insulin-induced inhibition of HGP. This suggests that activated KCs and factors they produce are unlikely inhibitors of insulin signalling in hepatocytes in the alcoholic liver.

In conclusion, our results confirm that alcohol consumption compromises glucose homoeostasis and demonstrate that it impairs hepatic insulin sensitivity. PPAR-$\alpha$ treatment that reduced steatosis and activation of NF-$\kappa$B-dependent pro-inflammatory pathways prevented hepatic insulin resistance, whereas KC depletion had little impact. These results favour the hypothesis that lipotoxicity and NF-$\kappa$B activation in hepatocytes, but not signals form professional inflammatory KCs, are involved in OH-induced hepatic insulin resistance.

## CLINICAL PERSPECTIVES

- Chronic alcohol consumption leads to liver steatosis and inflammation, and is a risk factor for cardiovascular diseases, diabetes and cancer. Those features and risk share insulin resistance as a common pathogenic threat.
- We demonstrated in the present study that alcohol induces hepatic insulin resistance in mice, and this was prevented by PPAR-$\alpha$ agonist treatment.
- If this translates to humans, it would be of importance to recognize and manage hepatic insulin resistance in alcoholic abusers as it may participate in liver disease progression and associated morbidity/mortality.

### AUTHOR CONTRIBUTION

Valérie Lebrun performed the experiments and drafted the paper. Olivier Molendi-Coste and Nicolas Lanthier participated in the clamp and liposome injection experiments respectively, and in the interpretation of the data. Christine Sempoux analysed the

histological sections. Patrice Cani supervised the clamp experiments and their analyses, and reviewed the paper. Nico van Rooijen prepared and provided the liposomes. Peter Starkel and Yves Horsmans participated in the study conception and design, data analysis and writing of the paper. Isabelle Leclercq conceived, designed and supervised the study, and wrote the paper.

**FUNDING**

The work was supported by D.G. Higher Education and Scientific Research of the French Community of Belgium (to I.A.L.), the Fund for Scientific Medical Research (Belgium) (to I.A.L.), and Astra Zeneca and Roche (to I.A.L. and Y.H.). I.A.L. and P.D.C. are FRS-FNRS Research Associates.

## REFERENCES

1 Mormone, E., George, J. and Nieto, N. (2011) Molecular pathogenesis of hepatic fibrosis and current therapeutic approaches. Chem. Biol. Interact. **193**, 225–231
2 Purohit, V., Gao, B. and Song, B. J. (2009) Molecular mechanisms of alcoholic fatty liver. Alcohol Clin. Exp. Res. **33**, 191–205
3 Stewart, S. F. and Day, C. P. (2003) The management of alcoholic liver disease. J. Hepatol. **38** Suppl. 1, S2–13
4 Browning, J. D. and Horton, J. D. (2004) Molecular mediators of hepatic steatosis and liver injury. J. Clin. Invest **114**, 147–152
5 Sakaguchi, S., Takahashi, S., Sasaki, T., Kumagai, T. and Nagata, K. (2011) Progression of alcoholic and non-alcoholic steatohepatitis: common metabolic aspects of innate immune system and oxidative stress. Drug Metab. Pharmacokinet. **26**, 30–46
6 Leclercq, I. (2013) Emerging concepts on pathogenesis of NASH. Non-alcoholic fatty liver disease: a Practical Guide, Wiley-Blackwell, Hoboken
7 Muoio, D. M. and Newgard, C. B. (2008) Mechanisms of disease: molecular and metabolic mechanisms of insulin resistance and $\beta$-cell failure in type 2 diabetes. Nat. Rev. Mol. Cell Biol. **9**, 193–205
8 Diehl, A. M., Li, Z. P., Lin, H. Z. and Yang, S. Q. (2005) Cytokines and the pathogenesis of non-alcoholic steatohepatitis. Gut **54**, 303–306
9 Patsouris, D., Li, P. P., Thapar, D., Chapman, J., Olefsky, J. M. and Neels, J. G. (2008) Ablation of CD11c-positive cells normalizes insulin sensitivity in obese insulin resistant animals. Cell Metab. **8**, 301–309
10 Lanthier, N., Molendi-Coste, O., Horsmans, Y., Van Rooijen, N., Cani, P. D. and Leclercq, I. A. (2010) Kupffer cell activation is a causal factor for hepatic insulin resistance. Am. J. Physiol.–Gastrointest. Liver Physiol. **298**, G107–G116
11 Nguyen, K. H., Lee, J. H. and Nyomba, B. L. (2012) Ethanol causes endoplasmic reticulum stress and impairment of insulin secretion in pancreatic $\beta$-cells. Alcohol **46**, 89–99
12 Kang, L., Sebastian, B. M., Pritchard, M. T., Pratt, B. T., Previs, S. F. and Nagy, L. E. (2007) Chronic ethanol-induced insulin resistance is associated with macrophage infiltration into adipose tissue and altered expression of adipocytokines. Alcohol Clin. Exp. Res. **31**, 1581–1588
13 Gao, B., Seki, E., Brenner, D. A., Friedman, S., Cohen, J. I., Nagy, L., Szabo, G. and Zakhari, S. (2011) Innate immunity in alcoholic liver disease. Am. J. Physiol. Gastrointest. Liver Physiol. **300**, G516–G525
14 Bradford, B. U., Enomoto, N., Ikejima, K., Rose, M. L., Bojes, H. K., Forman, D. T. and Thurman, R. G. (1999) Peroxisomes are involved in the swift increase in alcohol metabolism. J. Pharmacol. Exp. Ther. **288**, 254–259
15 Thakur, V., McMullen, M. R., Pritchard, M. T. and Nagy, L. E. (2007) Regulation of macrophage activation in alcoholic liver disease. J. Gastroenterol. Hepatol. **22** Suppl. 1, S53–S56
16 Koop, D. R., Klopfenstein, B., Iimuro, Y. and Thurman, R. G. (1997) Gadolinium chloride blocks alcohol-dependent liver toxicity in rats treated chronically with intragastric alcohol despite the induction of CYP2E1. Mol. Pharmacol. **51**, 944–950
17 Adachi, Y., Bradford, B. U., Gao, W., Bojes, H. K. and Thurman, R. G. (1994) Inactivation of Kupffer cells prevents early alcohol-induced liver injury. Hepatology **20**, 453–460
18 Thurman, R. G. (1998) II. Alcoholic liver injury involves activation of Kupffer cells by endotoxin. Am. J. Physiol. **275**, G605–G611
19 Bautista, A. P. (2000) Impact of alcohol on the ability of Kupffer cells to produce chemokines and its role in alcoholic liver disease. J. Gastroenterol. Hepatol. **15**, 349–356
20 Petrasek, J., Mandrekar, P. and Szabo, G. (2010) Toll-like receptors in the pathogenesis of alcoholic liver disease. Gastroenterol. Res. Pract. **2010**, 710381
21 Yan, A. W., Fouts, D. E., Brandl, J., Stärkel, P., Torralba, M., Schott, E., Tsukamoto, H., Nelson, K. E., Brenner, D. A. and Schnabl, B. (2011) Enteric dysbiosis associated with a mouse model of alcoholic liver disease. Hepatology **53**, 96–105
22 Hritz, I., Mandrekar, P., Velayudham, A., Catalano, D., Dolganiuc, A., Kodys, K., Kurt-Jones, E. and Szabo, G. (2008) The critical role of toll-like receptor (TLR) 4 in alcoholic liver disease is independent of the common TLR adapter MyD88. Hepatology **48**, 1224–1231
23 Burcelin, R., Dolci, W. and Thorens, B. (2000) Portal glucose infusion in the mouse induces hypoglycemia: evidence that the hepatoportal glucose sensor stimulates glucose utilization. Diabetes **49**, 1635–1642
24 van Rooijen, N. and Sanders, A. (1994) Liposome mediated depletion of macrophages: mechanism of action, preparation of liposomes and applications. J. Immunol. Methods **174**, 83–93
25 Lanthier, N., Molendi-Coste, O., Cani, P. D., Van Rooijen, N., Horsmans, Y. and Leclercq, I. A. (2011) Kupffer cell depletion prevents but has no therapeutic effect on metabolic and inflammatory changes induced by a high-fat diet. FASEB J. **25**, 4301–4311
26 Everard, A., Geurts, L., Van, R. M., Delzenne, N. M. and Cani, P. D. (2012) Tetrahydro iso-$\alpha$ acids from hops improve glucose homeostasis and reduce body weight gain and metabolic endotoxemia in high-fat diet-fed mice. PLoS ONE **7**, e33858
27 Leclercq, I. A., Farrell, G. C., Field, J., Bell, D. R., Gonzalez, F. J. and Robertson, G. R. (2000) CYP2E1 and CYP4A as microsomal catalysts of lipid peroxides in murine nonalcoholic steatohepatitis. J. Clin. Invest. **105**, 1067–1075
28 Leclercq, I. A., Lebrun, V. A., Stärkel, P. and Horsmans, Y. J. (2007) Intrahepatic insulin resistance in a murine model of steatohepatitis: effect of PPAR$\gamma$ agonist pioglitazone. Lab. Invest. **87**, 56–65
29 Mandrekar, P. and Szabo, G. (2009) Signalling pathways in alcohol-induced liver inflammation. J. Hepatol. **50**, 1258–1266
30 Farrell, G. C. (2005) Signalling links in the liver: knitting SOCS with fat and inflammation. J. Hepatol. **43**, 193–196
31 Leclercq, I. A., Da Silva, M. A., Schroyen, B., Van, H. N. and Geerts, A. (2007) Insulin resistance in hepatocytes and sinusoidal liver cells: mechanisms and consequences. J. Hepatol. **47**, 142–156
32 Moriya, T., Naito, H., Ito, Y. and Nakajima, T. (2009) 'Hypothesis of seven balances': molecular mechanisms behind alcoholic liver diseases and association with PPAR$\alpha$. J. Occup. Health **51**, 391–403

 

33 Kong, L., Ren, W., Li, W., Zhao, S., Mi, H., Wang, R., Zhang, Y., Wu, W., Nan, Y. and Yu, J. (2011) Activation of peroxisome proliferator activated receptor $\alpha$ ameliorates ethanol induced steatohepatitis in mice. Lipids Health Dis. **10**, 246

34 Chou, C. J., Haluzik, M., Gregory, C., Dietz, K. R., Vinson, C., Gavrilova, O. and Reitman, M. L. (2002) WY14,643, a peroxisome proliferator-activated receptor $\alpha$ (PPAR$\alpha$) agonist, improves hepatic and muscle steatosis and reverses insulin resistance in lipoatrophic A-ZIP/F-1 mice. J. Biol. Chem. **277**, 24484–24489

35 Vanden Berghe, W., Vermeulen, L., Delerive, P., De, B. K., Staels, B. and Haegeman, G. (2003) A paradigm for gene regulation: inflammation, NF-$\kappa$B and PPAR. Adv. Exp. Med. Biol. **544**, 181–196

36 Lanthier, N., Horsmans, Y. and Leclercq, I. A. (2010) Clodronate liposomes: all sites of injection are not equal. Hepatology **51**, 721–722

37 Onishi, Y., Honda, M., Ogihara, T., Sakoda, H., Anai, M., Fujishiro, M., Ono, H., Shojima, N., Fukushima, Y., Inukai, K., Katagiri, H. et al. (2003) Ethanol feeding induces insulin resistance with enhanced PI 3-kinase activation. Biochem. Biophys. Res. Commun. **303**, 788–794

38 Wan, Q., Liu, Y., Guan, Q., Gao, L., Lee, K. O. and Zhao, J. (2005) Ethanol feeding impairs insulin-stimulated glucose uptake in isolated rat skeletal muscle: role of Gs $\alpha$ and cAMP. Alcohol Clin. Exp. Res. **29**, 1450–1456

39 Cani, P. D., Bibiloni, R., Knauf, C., Waget, A., Neyrinck, A. M., Delzenne, N. M. and Burcelin, R. (2008) Changes in gut microbiota control metabolic endotoxemia-induced inflammation in high-fat diet-induced obesity and diabetes in mice. Diabetes **57**, 1470–1481

40 Nakajima, T., Kamijo, Y., Tanaka, N., Sugiyama, E., Tanaka, E., Kiyosawa, K., Fukushima, Y., Peters, J. M., Gonzalez, F. J. and Aoyama, T. (2004) Peroxisome proliferator-activated receptor $\alpha$ protects against alcohol-induced liver damage. Hepatology **40**, 972–980

41 Adachi, Y., Moore, L. E., Bradford, B. U., Gao, W. and Thurman, R. G. (1995) Antibiotics prevent liver injury in rats following long-term exposure to ethanol. Gastroenterology **108**, 218–224

42 Yin, M., Bradford, B. U., Wheeler, M. D., Uesugi, T., Froh, M., Goyert, S. M. and Thurman, R. G. (2001) Reduced early alcohol-induced liver injury in CD14-deficient mice. J. Immunol. **166**, 4737–4742

**Received 8 February 2013/7 June 2013; accepted 12 June 2013**

**Published as Immediate Publication 12 June 2013, doi: 10.1042/CS20130064**

Clinical Science (2013) **125**, 501–511 (Printed in Great Britain) doi: 10.1042/CS20130064

online data

Original Paper

## SUPPLEMENTARY ONLINE DATA

# Impact of PPAR-$\alpha$ induction on glucose homoeostasis in alcohol-fed mice

Valérie LEBRUN*, Olivier MOLENDI-COSTE*[1], Nicolas LANTHIER*, Christine SEMPOUX*†, Patrice D. CANI‡, Nico VAN ROOIJEN§, Peter STÄRKEL*, Yves HORSMANS* and Isabelle A. LECLERCQ*

*Laboratory of Hepato-Gastroenterology, Institut de Recherche Expérimentale et Clinique (IREC), Université catholique de Louvain, 1200 Brussels, Belgium
†Pathology Department, Cliniques Universitaires Saint-Luc, Université catholique de Louvain, 1200 Brussels, Belgium
‡Louvain Drug Research Institute, Metabolism and Nutrition research group, Université catholique de Louvain, 1200 Brussels, Belgium
§Department of Molecular Cell Biology, Vrije Universiteit Medical Center, 1081 Amsterdam, The Netherlands

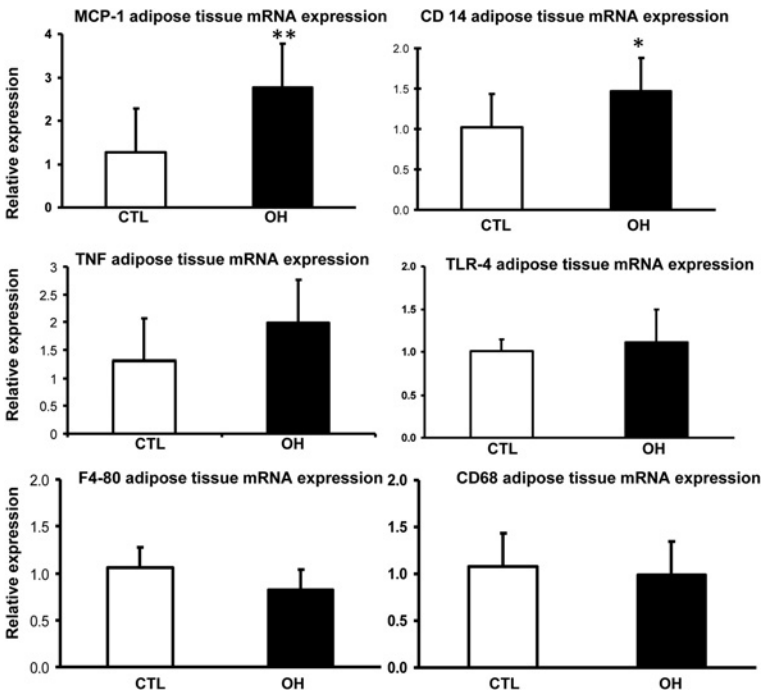


**Figure S1 Relative mRNA expression of MCP-1, CD14, TNF$\alpha$, TLR-4, F4/80 and CD68 in the epididymal adipose tissue of pair-fed controls and OH-fed mice**

Values are as mean + S.D., $n = 5$ per group. Mean value in adipose from pair-fed controls is arbitrarily set at 1. *$P < 0.05$ and **$P < 0.01$.

[1]**Present address:** UMR 1011 (Team 3), Institut Pasteur de Lille, 1 rue du professeur Calmette, BP245–59019–Lille, France

**Correspondence:** Professor Isabelle A. Leclercq (email isabelle.leclercq@uclouvain.be).

**Table S1 Primer sequences used for real-time RT–PCR analyses**

| Gene | Sequence | Primer | GenBank® |
|---|---|---|---|
| RPL-19 | Forward | GAAGGTCAAAGGGAATGTGTTCA | NM_009078 |
| | Reverse | CCTTGTCTGCCTTCAGCTTGT | |
| TNF-$\alpha$ | Forward | CCACCACGCTCTTCTGTCTAC | NM_013693 |
| | Reverse | TGGGCTACAGGCTTGTCACT | |
| IL-6 | Forward | CTGCAAGAGACTTCCATCCAGTT | NM_031168 |
| | Reverse | GAAGTAGGGAAGGCCGTGG | |
| TLR-4 | Forward | GCAGCAGGTGGAATTGTATCG | NM_021297 |
| | Reverse | TGTGCCTCCCCAGAGGATT | |
| F4/80 | Forward | GATGAATTCCCGTGTTGTTGGT | NM_010130 |
| | Reverse | ACATCAGTGTTCCAGGAGACACA | |
| CD 11b | Forward | GGGTCATTCGCTACGTAATTGG | NM_009605 |
| | Reverse | TGTTCACCAGCTGGCTTAGATG | |
| CD 11c | Forward | ACGTCAGTACAAGGAGATGTTGGA | NM_021334 |
| | Reverse | ATCCTATTGCAGAATGCTTCTTTACC | |
| CD 14 | Forward | CCTGCCCTCTCCACCTTAGAC | NM_009841 |
| | Reverse | TCAGTCCTCTCTCGCCCAAT | |
| CD 68 | Forward | TGCGGCTCCCTGTGTGT | NM_009853 |
| | Reverse | TCTTCCTCTGTTCCTTGGGCTAT | |
| CD 36 | Forward | GCCAAGCTATTGCGACATGA | NM_007643 |
| | Reverse | GAAAAGAATCTCAATGTCCGAGACT | |
| FAS | Forward | GATCCTGGAACGAGAACACGAT | NM_007988 |
| | Reverse | AGAGACGTGTCACTCCTGGACTT | |
| SREBP-1 | Forward | CTGGCACTAAGTGCCCTCAAC | NM_011480 |
| | Reverse | GCCACATAGATCTCTGCCAGTGT | |
| SCD-1 | Forward | CCAGAATGACGTGTACGAATGG | NM_009127 |
| | Reverse | GCGTGTGTTTCTGAGAACTTGTG | |
| ChREBP | Forward | GGACAAGATCCGG CTGAACA | AF156604 |
| | Reverse | GCTTCTCGTCCGTTGCACAT | |
| GPAT-1 | Forward | GTCCTGCGCTATCATGTCCA | NM_008149 |
| | Reverse | GGATTCCCTGCCTGTGTCTG | |
| DGAT-2 | Forward | ACTCTGGAGGTTGGCACCAT | NM_026384 |
| | Reverse | GGGTGTGGCTCAGGAGGAT | |
| SOCS-3 | Forward | CGGACCAGCGCCACTTC | NM_007707.2 |
| | Reverse | TCACACTGGATGCGTAGGTTCT | |
| PPAR-$\alpha$ | Forward | CAACGGCGTCGAAGACAAA | NM_011144 |
| | Reverse | TGACGGTCT CCACGGACAT | |

**Table S2 Antibodies used for Western blotting**

| Protein | Diluant | Molecular mass (kDa) | Primary antibody | Secondary antibody | Source |
|---|---|---|---|---|---|
| p-IR | Milk | 90 | 1:1000 | Rabbit (1:40 000) | Santa Cruz Biotechnology |
| IR | Milk | 90 | 1:1000 | Rabbit (1:40 000) | Santa Cruz Biotechnology |
| p-Akt (Ser) | BSA | 55 | 1:1000 | Rabbit (1:20 000) | Cell Signaling |
| p-Akt (Thr) | BSA | 55 | 1:1000 | Rabbit (1:20 000) | Cell signaling |
| Akt | Milk | 59 | 1:2000 | Mouse (1:20 000) | BD Transduction |
| p-ERK | Milk | 42/44 | 1:1000 | Mouse (1:20 000) | Cell Signaling |
| ERK | Milk | 42/44 | 1:1000 | Mouse (1:20 000) | BD Transduction |

**Table S3 Body and liver weight, food consumption and glycaemia in OH-fed mice treated with PBS- (OH PBS) and clodronate-loaded liposomes (OH clodronate)**

No significant differences were observed between the two groups.

| Parameter | OH-PBS ($n = 6$) | OH-clodronate ($n = 5$) |
|---|---|---|
| Body weight (g) | | |
| Day 0 | 18.6 ± 1.3 | 18.9 ± 1.0 |
| Day 21 | 17.1 ± 1.4 | 16.7 ± 1.4 |
| Liver weight (g) | 0.92 ± 0.07 | 0.94 ± 0.09 |
| Liver/body weight (%) | 5.34 ± 0.25 | 5.65 ± 0.73 |
| Liquid food consumption (ml/day) | 9.5 ± 0.6 | 9 ± 0.5 |
| Glycaemia (mg/dl) | 134.7 ± 16.2 | 118.8 ± 28.0 |

**Received 8 February 2013/7 June 2013; accepted 12 June 2013**

**Published as Immediate Publication 12 June 2013, doi: 10.1042/CS20130064**